APPLICATION NOTE

AN1302: Characterization of hyaluronic acid with online multi-angle light scattering and differential viscometry

Jason Waters, Wyatt Technology, and Danielle Leiske, Oregon State University

Introduction

Hyaluronic acid (HA) is a naturally occurring, unbranched polysaccharide that consists of alternately repeating D-glucuronic acid and N- acetylglucosamine units. This biopolymer is present throughout all mammalian systems but occurs primarily in synovial (joint) fluid, vitreous humor, and various loose connective tissues (such as rooster comb) (1). HA is of enormous commercial interest for ophthalmic, medical, pharmacological, and cosmetic applications.

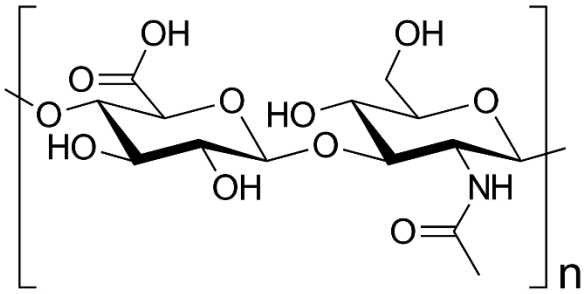

Figure 1. Hyaluronic acid is a natural polymer important in biology and commercial applications.

Hyaluronic acid has been studied extensively (1–7). The physiochemical behavior of HA has been tied closely to material characteristics such as the weight-average molecular weight (M_w), molecular weight distribution (also known as polydispersity index [PDI]), intrinsic viscosity ([η]), and molecular conformation.

Past studies of HA have included many size-exclusion chromatography (SEC) experiments. Traditional SEC involves chromatographically separating samples, monitoring the output with a concentration detector such as a refractometer or UV absorbance detector and relating the elution time to molar mass. SEC in this form is a purely relative measurement, because the chromatographic system must first be calibrated with a series of known molar mass standards to produce a calibration curve. The accuracy of the calibration depends on the analyte having the same conformation and column interactions as the reference standards.

Other SEC studies of HA have added multiangle light-scattering (MALS) devices in series with concentration detectors. This proves advantageous because SEC-MALS is an extremely sensitive technique for measuring absolute molar masses that does not rely on calibration standards or a priori assumptions about the molecular conformation. With SEC-MALS one also can determine a sample's root mean-square radius R_g, provided the sample R_g is greater than about 10 nm.

The Mendichi group at the Istituto di Chimica delle Macromolecole (Milan, Italy) performed a number of elegant experiments involving SEC-MALS of HA with the addition of online, single-capillary viscometry (2,3). This combination of detectors yields not only all of the aforementioned material characteristics but also elucidates sample intrinsic viscosity and, using the Mark–Houwink–Sakurada (MHS) relationship, molecular conformation.

However, single-capillary viscometry is inherently vulnerable to noise generated by system pressure fluctuations. Even using a pulse-free pump and Fourier-transform data filtering, single-capillary viscometry detector S/N of only approximately 125:1 has been shown (8,9). Another drawback of this technique is its reliance on calibration using a large number of known standards.

Differential viscometry is particularly advantageous as compared with single-capillary viscometry, as will be shown. In this application note we present SEC-MALS-IV for absolute determination of HA properties using MALS, differential refractometry, and differential viscometry detectors in series with SEC separation.

Materials and Methods

Samples

Seven distinct HA samples were used for this study. HA sources included rooster comb, umbilical cord, and bacterial fermentation. Ovalbumin was obtained from Sigma (St. Louis, Missouri). All other chemicals were analytical grade.

Analytical instruments

The chromatographic system consisted of an HPLC system and autoinjector (Agilent 1100], 900 µL injection loop) with a solvent degasser (ERC L761). The SEC column system consisted of a Polymer Labs Aquagel- OH (8 µm) separation column with guard column. The mobile phase was phosphate-buffered saline (PBS, 8 mM dibasic sodium phosphate, 22 mM monobasic sodium phosphate, 150 mM sodium chloride in doubly deionized water). The flow rate was 0.5 mL/min. Chromatographic detectors included a DAWN® MALS device, a ViscoStar® differential viscometer, and an Optilab® differential refractometer in series.

All solution concentrations were 0.1 mg/mL HA in PBS. The injection volume was 900 µL. The *dn/dc* value for HA, 0.167 mL/g, was taken from the literature (1). The low concentration and large injected volume were selected to avoid potential viscous-fingering of HA samples within the separation column. Injections were performed multiple times for each sample to verify repeatability of results.

The MALS detector determines absolute molar mass without the need for reference standards, column calibration, or "fudge factors." The differential refractometer was used for concentration measurements. Thermal control via a Peltier device allows for thermal stability at or below room temperature, and thus stable baselines and extremely high S/N.

Differential viscometry

The differential viscometer uses the traditional four-arm capillary bridge design (Figure 2). The bridge is composed of four equal-impedance capillaries with the lower-left arm possessing an effectively zero-impedance delay volume. As mobile phase propagates through the device, the differential pressure (ΔP) transducer in the center of the bridge reads zero. When the sample enters the bridge, it splits evenly. When the sample enters the delay volume, three capillaries contain sample and one contains only mobile phase. This creates a pressure imbalance within the bridge that is detected by ΔP. The sample specific viscosity (η_{sp}) can be directly determined from the combination of the ΔP pressure imbalance and the device inlet pressure (IP) by means of the following relationship, derived from the Stokes–Einstein equation (10):

$$\eta_{sp} = \frac{\eta}{\eta_0} - 1 = \frac{4\Delta P}{IP - 2\Delta P} \quad [2]$$

where η is the sample viscosity and η_0 the solvent viscosity.

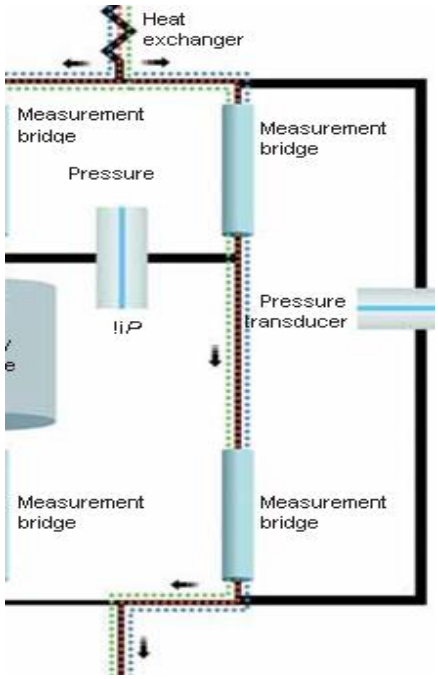

Figure 2. Schematic of the differential viscometer design.

This is a direct measurement that depends only upon calibrated pressure transducers. The bridge design is inherently insensitive to pressure fluctuations and thus is able to tolerate moderate pump pulses. Additionally, the device utilizes a Peltier thermoelectric device for precision thermal control within a large temperature range, including at or below room temperature. The combination of bridge design, precise thermal control, and contemporary electronics results in a device with outstanding S/N.
A more advanced design is described in ViscoStar: Innovations in Online Viscometry for GPC.

Data analysis

Experimental collection and data analysis were performed with the ASTRA software package (Wyatt Technology).

Using this software, we were able to collect and subsequently analyze all 18 MALS angles along with the ΔP, IP, and differential refractometry signals.

Knowledge of both η_{sp} as determined by the differential viscometer and concentration c as determined by the differential refractometer allow for the direct calculations of intrinsic viscosity $[\eta]$ using Equation 3, which is applied to every data slice across an elution peak.

$$[\eta] = \lim_{c \to 0} \eta_{sp}/c \qquad [3]$$

The MALS detector provides molar mass data at each data slice as well, so the entire distribution can be fit to the MHS equation,

$$[\eta] = KM^a \qquad [4]$$

where M is molecular weight and K and a are MHS coefficients that correspond to polymer shape and solvent interaction. The a value in particular is an indicator of polymer shape in solution, with lower a values (for example, $a < 0.5$) indicating more compact conformations and higher a values (for example, $a > 0.8$) indicating extended conformations.

The hydrodynamic volume V_h of the sample also can be determined from MALS and viscometry measurements by means of the Einstein–Simha relation:

$$V_h = \frac{M[\eta]}{2.5N_A} \qquad [5]$$

where N_A is Avogadro's number. The viscometric hydrodynamic radius R_h is calculated as

$$R_h = (3\,V_h/4\pi)^{1/3}. \qquad [6]$$

Defined this way, R_h is the radius of a sphere that has the same $[\eta]$ as the sample.

Band-broadening correction

As the sample travels through the detectors, each flow cell acts like a small mixing volume. These discrete mixing chambers cause an initially sharp peak to broaden with a slight exponential tail. Left uncorrected, this causes experimental results to be slightly distorted (10). Band broadening is present whenever more than one detector is used for HPLC detection. The software utilizes a proprietary band-broadening correction algorithm, which solves the long-standing problem of inter-detector band broadening.

Results and Discussion

Table I summarizes the material characteristics determined for the seven HA samples. Results are in agreement with published values (1–3,5).

Figure 3 shows a typical η_{sp} chromatogram of an HA sample along with the associated M_w, R_g, and R_h values across the peak. The typical differential viscometer S/N of the η_{sp} trace for these HA experiments was on the order of 2200:1, more than one order of magnitude better than pulse-free, data-filtered single-capillary viscometry.

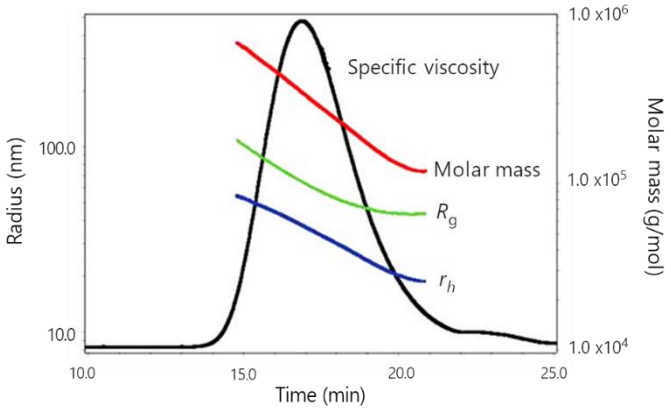

Figure 3. η_{sp} chromatogram of sample HA-2 with associated M_w, R_g, and R_h values across the peak.

To evaluate molecular conformation information, MHS plots were constructed for all samples. See Figure 4 for a representative MHS plot of sample HA-2. The least-squares regression of the MHS trace also can be seen in Figure 4. From this regression, the K and a values for sample HA-2 were calculated as K=0.0277 and a = 0.817, both values being close to published values. However, these numbers should not be taken at face value, as it can be seen that the MHS trace shows marked curvature. Though not shown, all seven HA samples tested within this study exhibited MHS curvature similar to that seen in Figure 3. Because all HA MHS plots show curvature, the K and a coefficients as determined by direct linear regression of MHS plots cannot be taken as accurate descriptors of MHS behavior across the entire span of HA molecular weights. Indeed, this is true of previously published K and a values.

By using a polynomial fit (in this case second order) of the MHS curve and subsequently taking the derivative of that function, one can determine instantaneous a values (a_i):

$$a_i = \mathrm{d}(\log[\eta])/\mathrm{d}(\log M). \qquad [7]$$

Table 1. Summary of HA sample material characteristics

HA Sample	HA Source	M_W (g/mol)	PDI	R_g (nm)	[η] (mL/g)	r_h (nm)
HA-1	Bacterial fermentation	2.64E+05	1.19	57.7	632	27.7
HA-2	Umbilical cord	2.84E+05	1.23	66.1	652	28.3
HA-3	Chicken comb	6.62E+05	1.10	109.1	1431	51.1
HA-4	Bacterial fermentation	1.10E+06	1.45	165.4	1754	57.7
HA-5	Umbilical cord	1.44E+06	1.06	180.4	2208	77.7
HA-6	Chicken comb	1.62E+06	1.06	182.4	2671	86.1
HA-7	" Natural sources"	1.76E+06	1.02	207.9	2655	89.9

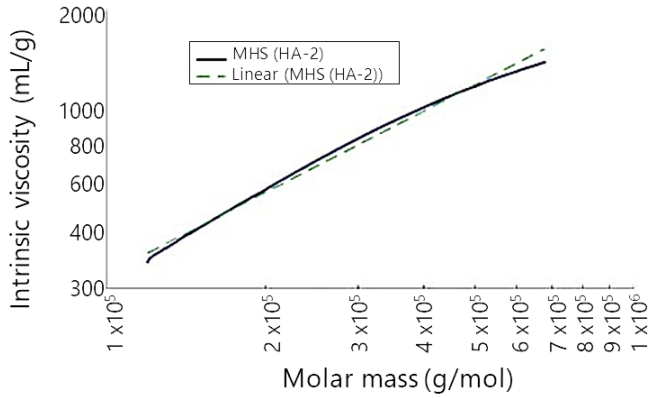

Figure 4. Mark–Houwink–Sakurada plot and linear fit for sample HA-2.

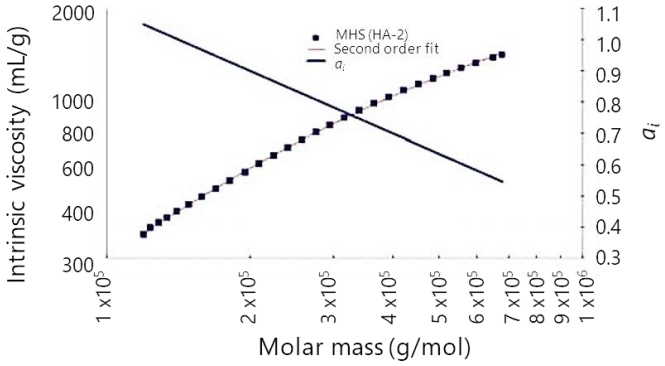

Figure 5. Mark–Houwink–Sakurada plot, second-order fit, and a_i versus log(M_w) for sample

Figure 5 presents the a_i values of sample HA-2, which range from 1.0 at lower molecular weights to nearly 0.55 at high molecular weights. The six other HA samples showed a_i behavior analogous to that described earlier, with typical a_i values ranging from 1.1 at low molecular weights to 0.5 at high molecular weights.

This variation in a across its molar mass range indicates that HA exhibits free-draining, non-Gaussian chain behavior at lower molecular weights (2). The inherent stiffness of this polyelectrolyte forces the molecule to take on a more extended conformation at lower molecular weights, and thus a correspondingly high a_i value. As molecular weight increases, HA slowly transitions into standard Gaussian chain behavior and a_i values drop. This might help explain the wide variety (and inconsistency) of HA MHS constants that have been published in the literature.

Conclusions

By combining a MALS instrument, a differential refractometer, and a differential viscometer with SEC, we have explored the material characteristics of the biopolymer HA. We have determined the absolute HA molecular weight, molecular weight distribution, and radii information to be consistent with historical literature values. HA molecular conformation, as elucidated by MHS analysis, has been found to exhibit unusual behavior, as shown previously by the Mendichi group. Utilization of these detectors in tandem with the software ensured rapid, accurate, absolute analysis of this behavior with unprecedented S/N and no need for calibration curves for any of the detectors.

References

(1) S. Hokputsa et al., *Eur. Biophys. J.* **32**, 450–496 (2003).

(2) R. Mendichi et al., *Biomacromolecules* **4**, 1805–1810 (2003).

(3) R. Mendichi and A. Giacometti Schieroni, *Polymer* **43**, 6115–6121.

(4) R. Mendichiet al., *Polymer* **39**, 6611–6620 (1998).

(5) L. Solteset al., *Biomed. Chromatogr.* **16**, 459–462 (2002).

(6) K. Kazuaki et al., *J. Chromatogr. B* **797**, 347–355 (2003).

(7) N. Berriaud et al., *Int. J. Biol. Macromolecules* **16**, 137–142 (1994).

(8) R. Mendichi and A. Giacometti Schieroni, *J. Appl. Polymer Sci.* **68**, 1651–1659 (1998).

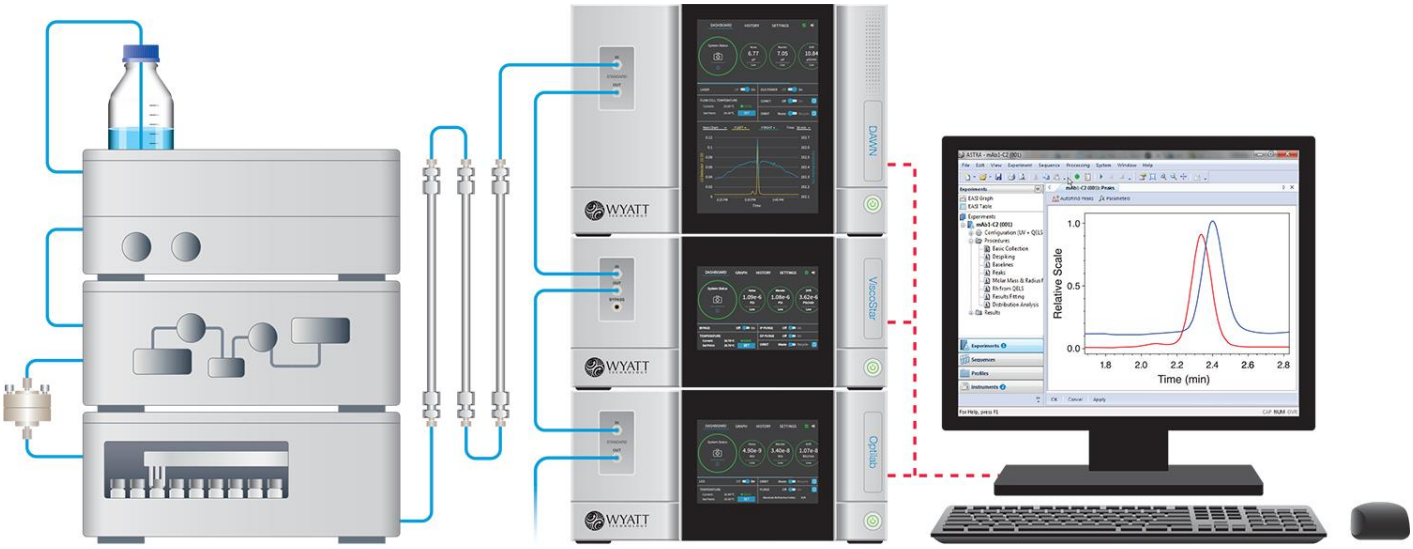

WYATT TECHNOLOGY